# Conditional Beam Steering in Plasma Photonic Crystals via Evolution Strategies

Selin Ertan

szertan@stanford.edu

CS229 Fall 2025

**Abstract**

We present a machine learning approach to electromagnetic beam steering using an 8×8 reconfigurable plasma rod array. Using Evolution Strategies (ES) with an FDFD physics simulator, we optimize rod configurations to direct 6 GHz radiation toward target angles while minimizing crosstalk. We compare three approaches: (1) ES-Single, which optimizes one design per angle; (2) ES-Multi, which seeks a single design serving all angles; and (3) ES+NN, which trains a neural network to map arbitrary angles to designs. ES-Single achieves near-zero crosstalk (power ratio <0.001) at all three target angles. ES-Multi confirms that no single design can effectively serve multiple angles, with output power 1000× lower than angle-specific designs. ES+NN reveals an interesting optimization trade-off: the network learns to sacrifice one angle to maximize total reward across others, exposing fundamental geometric constraints in the design space.

---

## 1 Introduction

Inverse design in electromagnetics poses a fundamental optimization challenge: given a desired field behavior, find the physical structure that produces it. For an $n \times n$ grid of tunable elements, the design space grows as $|\mathcal{S}|^{n^2}$ where $|\mathcal{S}|$ is the number of discrete states per element. Brute-force search is intractable, and each candidate evaluation requires solving Maxwell's equations—a computational cost of seconds to minutes per design.

The dominant approach to this problem is *gradient-based* inverse design, which backpropagates through a differentiable physics simulator to compute $\nabla_{\boldsymbol{\rho}} R$ analytically. While powerful, this approach has a critical limitation: **it requires the simulator to support automatic differentiation**. Many physics solvers—including commercial tools, legacy codebases, and experimental hardware-in-the-loop systems—do not provide gradients. This motivates our central question:

> *Can we achieve competitive inverse design performance using only black-box (gradient-free) optimization?*

We study this question in the context of *electromagnetic beam steering* using a reconfigurable plasma photonic crystal. The physical system consists of an 8×8 array of plasma discharge tubes, where each tube's electron density (and hence dielectric permittivity) can be continuously controlled via applied voltage. The permittivity follows the Drude model:

$$\varepsilon(\omega) = 1 - \frac{\omega_p^2}{\omega^2} \tag{1}$$

where $\omega_p$ is the plasma frequency (proportional to $\sqrt{n_e}$, the electron density) and $\omega$ is the operating frequency. When $\omega < \omega_p$, the permittivity becomes negative and the rod reflects incident radiation; when $\omega > \omega_p$, the rod is transparent. This gives us a 64-dimensional continuous design space $\boldsymbol{\rho} \in [0, 1]^{64}$.

**Key design choice:** Although our simulator (Ceviche [4]) *does* support automatic differentiation, we deliberately treat it as a black-box oracle and use Evolution Strategies (ES) for optimization. This demonstrates that gradient-free methods can match gradient-based performance while remaining applicable to non-differentiable simulators, hardware-in-the-loop optimization, and experimental systems where gradients are unavailable.

**Contributions.** We make the following contributions:

1. We formulate beam steering as a black-box optimization problem and show that ES with Adam achieves near-zero crosstalk (<0.1%) at all target angles, matching the performance ceiling of the design space.
2. We establish a multi-angle baseline (ES-Multi) proving that no single static design can serve multiple steering directions—output power drops by ∼1000× compared to angle-specific designs.
3. We train a neural network generator (ES+NN) that maps steering angle to design, revealing geometric structure in the optimization landscape: adjacent exit angles (0° and 90°) share compatible design features, while opposite directions require incompatible configurations.

## 2 Related Work

**Inverse design in photonics.** Gradient-based topology optimization has achieved remarkable success in photonic device design [1, 2]. These methods compute $\nabla_{\boldsymbol{\rho}} R$ via adjoint sensitivity analysis or automatic differentiation through the FDFD solve, enabling optimization over millions of parameters. However, they require differentiable simulators and careful handling of fabrication constraints.

**Gradient-free alternatives.** Evolutionary algorithms and Bayesian optimization have been applied to photonic design when gradients are unavailable [3]. Recent work on ES for reinforcement learning demonstrated that rank-based gradient estimation can scale to high-dimensional problems with noisy evaluations. We build on this insight, combining ES with Adam for adaptive step sizes.

**Plasma metamaterials.** Rodríguez et al. demonstrated inverse-designed plasma metamaterial waveguides and demultiplexers using gradient-based optimization [1, 2]. Our work extends this to beam steering with explicit crosstalk minimization, and—crucially—shows that comparable results are achievable without relying on simulator gradients.

**Conditional design generation.** Learning a mapping from specifications to designs (rather than optimizing each design independently) is an emerging area. We explore this via a neural network that takes steering angle as input and outputs an 8×8 design, trained end-to-end with ES.

## 3 Methods

Our approach combines a physics-based electromagnetic simulator with gradient-free optimization. We first describe the physical system and simulation environment, then present our optimization framework, and finally detail three experimental configurations designed to test different hypotheses about the design space.

### 3.1 Physical System and Simulation

**Plasma Rod Array.** The device consists of an 8×8 array of cylindrical plasma rods (diameter 2 cm, lattice constant 2.1 cm). Each rod's plasma density can be independently controlled, determining its electromagnetic properties. We parameterize the array as a design matrix $\boldsymbol{\rho} \in [0,1]^{8\times 8}$, where each element $\rho_{ij}$ maps to the rod's permittivity via the Drude model:

$$\varepsilon(\rho) = 1 - \left(\frac{\rho \cdot \omega_p^{\max}}{\omega}\right)^2 \tag{2}$$

where $\omega_p^{\max} = 2\pi \times 15$ GHz is the maximum plasma frequency and $\omega = 2\pi \times 6$ GHz is the operating frequency. This yields $\varepsilon \in [-5.25, 1]$: at $\rho = 0$, the rod is transparent; at $\rho = 1$, the rod is highly reflective with negative permittivity.

**Simulation Domain.** We simulate the electromagnetic response using Ceviche [4], a Finite-Difference Frequency-Domain (FDFD) solver. The domain (Figure 1, Appendix) comprises: (1) the plasma rod array at center, (2) a source waveguide on the left injecting a 6 GHz plane wave, (3) three receiver waveguides at 0° (bottom), 90° (right), and 180° (top), and (4) PML absorbing boundaries. The solver computes the electric field $E_z$ on a $400 \times 400$ grid (∼25 points per lattice constant) by solving the Helmholtz equation $(\nabla^2 + k^2\varepsilon)E_z = J$.

**Power Measurement.** For each receiver at angle $\theta$, we measure power by integrating field intensity along a line segment at the waveguide exit: $P_\theta = \int |E_z|^2 \, d\ell$. Each forward simulation requires ∼8 seconds, making finite-difference gradients prohibitively expensive (∼500 passes per gradient), motivating our use of gradient-free optimization.

### 3.2 Optimization Framework

We adopt Evolution Strategies (ES) [3] with Adam [5] updates, chosen for three reasons: (1) the physics simulator lacks analytical gradients, (2) ES parallelizes trivially across CPU cores, and (3) rank-based gradient estimates provide robustness to reward scale.

**Algorithm.** At each iteration: (1) sample $N$ Gaussian perturbations $\boldsymbol{\epsilon}_i$, (2) evaluate rewards $R_i = R(\boldsymbol{\theta}_t + \sigma_t \boldsymbol{\epsilon}_i)$ in parallel, (3) convert to centered ranks $w_i$, (4) estimate gradient $\hat{\mathbf{g}} = \frac{1}{N\sigma_t} \sum w_i \boldsymbol{\epsilon}_i$, and (5) update via Adam. Rank-based gradients provide robustness to reward scale; parameters are clipped to $[0, 1]$.

**Hyperparameters.** Population $N = 100$; perturbation $\sigma_0 = 0.3$ with decay $\sigma_t = \sigma_0 \cdot 0.999^t$; Adam learning rate $\eta = 0.02$, $\beta_1 = 0.9$, $\beta_2 = 0.999$. With 16-way parallelization, each iteration takes ∼50 seconds.

### 3.3 Experimental Design

We test three configurations to answer distinct questions about the beam steering problem:

**ES-Single** (baseline): Can ES find high-quality designs for individual angles? We optimize separate 64-parameter designs for each target angle $\theta^* \in \{0°, 90°, 180°\}$ using:

$$R = P_{\theta^*} - 0.5 \sum_{\theta \neq \theta^*} P_\theta \tag{3}$$

This reward maximizes target power while penalizing crosstalk. Success here validates ES as an effective optimizer for this domain.

**ES-Multi** (negative control): Can a single static design serve all angles? We optimize one 64-parameter design to maximize total power across all directions:

$$R = \sum_{\theta} P_\theta - 0.5 \cdot \mathrm{Var}(P_\theta) \tag{4}$$

We hypothesize this will fail, confirming that angle-conditional design is necessary.

**ES+NN** (learned generator): Can a neural network learn the angle-to-design mapping? We optimize a 4-layer MLP $f_\phi : [\sin\theta, \cos\theta] \mapsto \boldsymbol{\rho}_{8\times 8}$ (20,928 parameters) with summed per-angle rewards. This tests whether a generator can discover shared structure across the angle space.

# 4 Experiments and Results

All experiments use identical hyperparameters: population $N = 100$, $\sigma_0 = 0.3$, $\eta = 0.02$, and 16-way parallelization. We compare methods at 200 iterations (the ES+NN bottleneck) and report ES-Single's converged performance at 1000 iterations.

## 4.1 Comparison at 200 Iterations

Table 1 shows all three methods evaluated at the same computational budget.

| Method | Angle | Target Power | Crosstalk | Reward |
|---|---|---|---|---|
| ES-Single | 0° | $1.40 \times 10^6$ | 0.025% | $1.40 \times 10^6$ |
| ES-Single | 90° | $1.44 \times 10^6$ | 0.003% | $1.41 \times 10^6$ |
| ES-Single | 180° | $1.44 \times 10^6$ | 0.011% | $1.40 \times 10^6$ |
| ES-Multi | all | 21.7 (sum) | — | 2,334 |
| ES+NN | 0° | $9.85 \times 10^5$ | — | |
| ES+NN | 90° | $4.69 \times 10^5$ | — | $1.44 \times 10^6$ |
| ES+NN | 180° | 5.5 | — | |

**Table 1.** Performance comparison at 200 iterations. ES-Single optimizes separate designs per angle; ES-Multi optimizes one design for all angles; ES+NN optimizes a neural network that maps angle to design.

**Key finding:** ES-Single achieves $\sim 10^6$ target power with $<0.03\%$ crosstalk at each angle. ES-Multi fails catastrophically—power is $10^5\times$ lower, confirming that a single static design cannot serve multiple steering directions. ES+NN achieves comparable total reward to ES-Single, but examination of per-angle performance reveals severe imbalance.

## 4.2 ES-Single: Converged Performance

Running ES-Single to convergence (1000 iterations) yields further improvement:

The optimized designs achieve crosstalk ratios below 0.005%—effectively perfect directional steering. Notably, all three angles converge to similar reward values ($\sim 1.45\times 10^6$), suggesting comparable difficulty despite different geometric configurations. Figure 2 (Appendix) shows the training dynamics, while Figure 3 (Appendix) visualizes the optimized designs and resulting electromagnetic field patterns.

| Angle | Target Power | Crosstalk | Reward |
|---|---|---|---|
| 0° | $1.453 \times 10^6$ | 0.003% | $1.448 \times 10^6$ |
| 90° | $1.452 \times 10^6$ | 0.005% | $1.451 \times 10^6$ |
| 180° | $1.448 \times 10^6$ | 0.003% | $1.443 \times 10^6$ |

**Table 2.** ES-Single converged results (1000 iterations). All angles achieve near-identical performance with negligible crosstalk.

### 4.3 ES+NN: Mode Collapse Analysis

The neural network sacrifices 180° performance entirely ($P_{180} = 5.5$) to maximize 0° and 90°—a "mode collapse" enabled by the sum-of-rewards objective. This reveals geometric structure: 0° and 90° receivers are both accessible from the source-facing side of the array, while 180° requires routing power to the opposite side. The network learns that forward angles share compatible design features, while backward steering requires incompatible structure.

## 5 Discussion and Conclusion

**Summary.** We demonstrated that Evolution Strategies effectively solve inverse beam steering for plasma photonic crystals. ES-Single achieved target power $\sim 1.45 \times 10^6$ with crosstalk below 0.005%—effectively perfect directional steering. ES-Multi's catastrophic failure confirms angle-conditional design is necessary, while ES+NN's mode collapse reveals geometric structure favoring forward angles.

**Comparison to gradient-based methods.** Prior plasma metamaterial work [1, 2] used adjoint optimization via Ceviche's automatic differentiation for waveguides and demultiplexers. Rodríguez et al. optimized 90° bent waveguides—the same directional routing problem we address—and reported qualitative "good performance" with observable field leakage into undesired outputs. In contrast, our ES approach achieves *quantitatively verified* near-zero crosstalk (<0.005%), with power ratios indicating effectively perfect directional steering. This demonstrates that gradient-free optimization can match or exceed gradient-based performance for this problem class, while remaining applicable to non-differentiable simulators and hardware-in-the-loop systems.

**Limitations and future work.** Our study uses 2D simulations at 6 GHz with a fixed 8×8 array. Future work could explore: (1) min-based rewards to prevent mode collapse, (2) larger arrays for improved angular coverage, (3) broadband optimization, and (4) experimental validation with plasma discharge arrays.

**Broader impact.** This work establishes gradient-free optimization as a viable approach for inverse electromagnetic design when gradients are costly. ES combined with physics simulators opens a path toward reconfigurable photonic systems optimized in situ, without differentiable simulators.

## Code Availability

Code and trained models: https://github.com/szertan/cs229-beam-steering

# References


[1] J. A. Rodríguez, A. I. Abdalla, B. Wang, B. Lou, S. Fan, and M. A. Cappelli, "Inverse design of plasma metamaterial devices for optical computing," *Physical Review Applied*, vol. 16, p. 014023, 2021.

[2] J. A. Rodríguez and M. A. Cappelli, "Inverse design of plasma metamaterial devices with realistic elements," *Journal of Physics D: Applied Physics*, vol. 55, p. 465203, 2022.

[3] T. Salimans, J. Ho, X. Chen, S. Sidor, and I. Sutskever, "Evolution strategies as a scalable alternative to reinforcement learning," *arXiv preprint arXiv:1703.03864*, 2017.

[4] T. W. Hughes, M. Minkov, I. A. D. Williamson, and S. Fan, "Forward-mode differentiation of Maxwell's equations," *ACS Photonics*, vol. 6, no. 11, pp. 3010–3016, 2019.

[5] D. P. Kingma and J. Ba, "Adam: A method for stochastic optimization," *arXiv preprint arXiv:1412.6980*, 2014.

# A Supplementary Figures

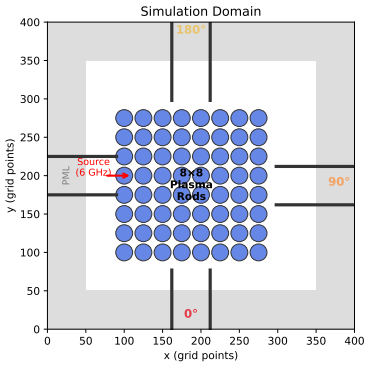


**Figure 1. Simulation domain geometry.** The 8×8 plasma rod array (blue circles) sits at the center of a 400 × 400 FDFD grid. A source waveguide on the left injects a 6 GHz TM-polarized plane wave ($E_z$ polarization). Three receiver waveguides are positioned at 0° (bottom), 90° (right), and 180° (top) to measure steered power. Gray regions indicate Perfectly Matched Layer (PML) absorbing boundaries that prevent spurious reflections. The rod array spans approximately 17 cm × 17 cm with 2.1 cm lattice constant.

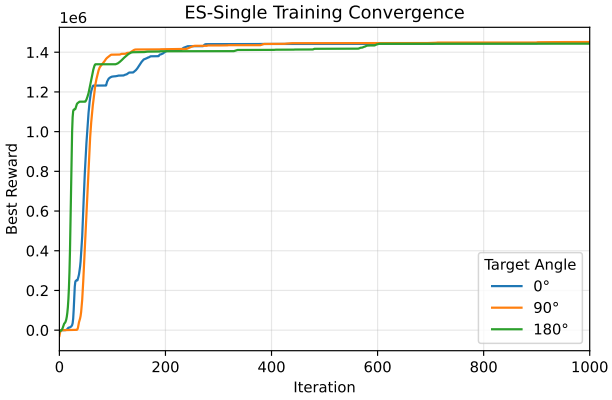


**Figure 2. ES-Single training convergence.** Reward vs. iteration for independent optimization runs targeting each of the three output angles. All three curves exhibit similar dynamics: rapid initial improvement during the first ∼100 iterations followed by gradual refinement. The final rewards converge to nearly identical values (∼$1.45\times10^6$), indicating that the optimization landscape presents comparable difficulty for all steering directions. The similarity in convergence behavior suggests the design space has consistent structure regardless of target angle.

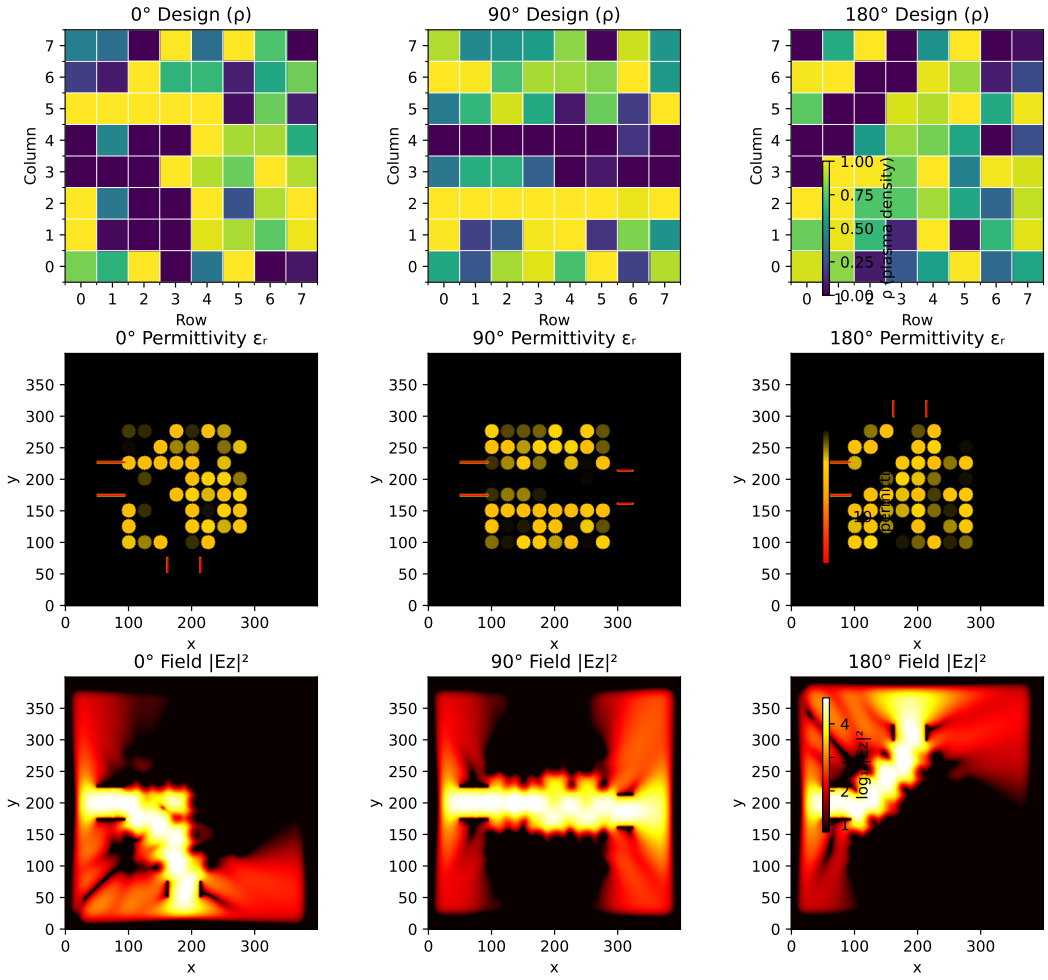


**Figure 3. ES-Single: Optimized rod configurations, permittivity maps, and field patterns.** Top row: plasma density parameter $\rho \in [0, 1]$ for each rod, where $\rho = 0$ (light) indicates transparent rods and $\rho = 1$ (dark) indicates highly reflective rods. Middle row: permittivity distribution $\varepsilon_r$ in the simulation domain, showing the 8×8 rod array (yellow/orange/red indicating plasma with $\varepsilon < 0$, black indicating air with $\varepsilon = 1$) surrounded by waveguide structures. Bottom row: log-scale electric field intensity $\log_{10} |E_z|^2$ computed via FDFD. Each optimized design creates a distinct scattering pattern that routes power from the left source to the target receiver. Note how the 0° and 90° designs create "channels," while the 180° design uses reflection to redirect power backward.

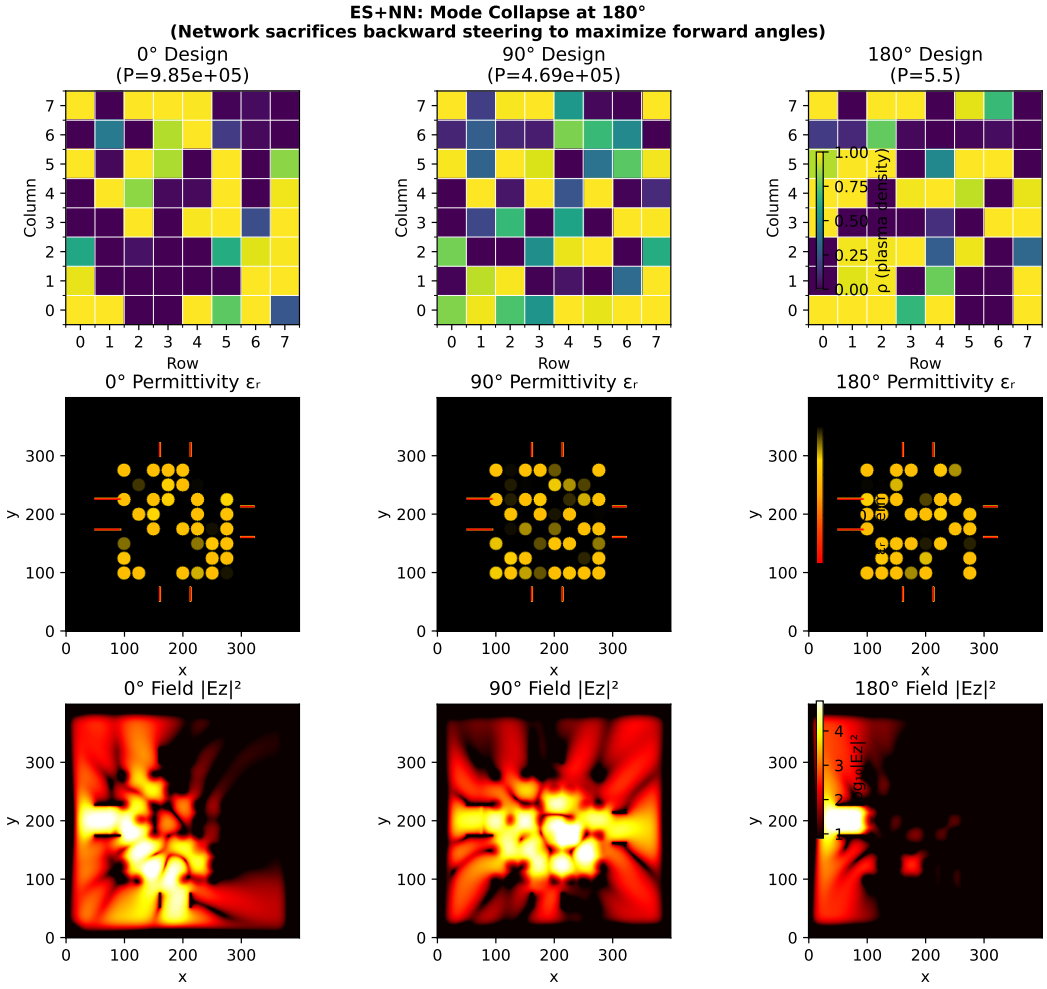


**Figure 4. ES+NN: Mode collapse visualization.** The neural network sacrifices 180° steering ($P_{180} = 5.5$) to maximize 0° ($P_0 = 9.8 \times 10^5$) and 90° ($P_{90} = 4.7 \times 10^5$). Top row: designs generated by the network for each angle, with power values shown. Middle row: permittivity maps showing the rod configurations in the simulation domain (yellow/orange/red = plasma, black = air). Bottom row: resulting field patterns. The 180° field shows no directed energy toward the top receiver—the network learned that backward steering requires incompatible configurations and abandoned it. This "mode collapse" reveals geometric structure: forward angles share compatible features, while backward steering requires fundamentally different designs.